Supporting Information

Kissling et al. (2012): Cenozoic imprints on the phylogenetic structure of palm species assemblages worldwide.

Table S1: Statistical results for testing whether the mean net relatedness index (NRI, response variable) for a given spatial extent (global, South America, Africa, Indomalaya, Australasia) and sampling pool (global, hemispheric, realm) differs significantly from zero. Significant results (i.e., non-random phylogenetic structure) are highlighted in **bold**. An intercept-only linear ordinary least squares (OLS) regression model was used to test whether the intercept significantly departs from zero (equivalent to a non-spatial one sample *t*-test). In the presence of spatial autocorrelation in OLS model residuals, a spatial model of the simultaneous autoregressive error type (SAR) was used instead (equivalent to a 'spatial' one sample *t*-test). SAR models were fitted with a row standardized coding scheme and a neighborhood based on a Gabriel connection (global spatial extent) or a minimum distance to connect each sample unit to at least one other site (South America, Africa, Indomalaya, Australasia). Moran's *I* values were used to assess residual spatial autocorrelation in OLS and SAR models based on the four nearest neighbors of each site. Significance of Moran's *I* statistics was determined from permutation tests (n = 1000 permutations). All Moran's *I* values of reported OLS and SAR models were not significant ($P > 0.05$).

Model				Results		
Spatial extent	Sample size	Sampling pool	Model type	Intercept (±SE)	*z* or *t*	*P*-value
Global	**152**	**global**	**SAR**	**3.842 (±0.752)**	**5.113**	**<0.001**
South America	**17**	**global**	**SAR**	**11.946 (±3.189)**	**3.746**	**<0.001**
South America	**17**	**hemispheric**	**SAR**	**6.806 (±2.152)**	**3.163**	**0.002**
South America	17	realm	SAR	1.164 (±1.415)	0.822	0.411
Africa	43	global	SAR	0.439 (±0.315)	1.393	0.164
Africa	43	hemispheric	SAR	0.038 (±0.283)	0.134	0.893
Africa	43	realm	SAR	0.475 (±0.320)	1.485	0.138
Indomalaya	**25**	**global**	**OLS**	**2.362 (±0.448)**	**5.266**	**<0.001**
Indomalaya	**25**	**hemispheric**	**OLS**	**1.066 (±0.349)**	**3.058**	**0.005**
Indomalaya	25	realm	OLS	0.375 (±0.280)	1.344	0.192
Australasia	**14**	**global**	**OLS**	**4.822 (±1.604)**	**3.007**	**0.010**
Australasia	**14**	**hemispheric**	**OLS**	**3.666 (±1.377)**	**2.663**	**0.020**
Australasia	14	realm	OLS	0.930 (±0.913)	1.019	0.327

Table S2: Insular geographic units (TDWG level 3 units) which show high phylogenetic clustering, i.e., the top 10 highest positive values of the net relatedness index (NRI) in palm assemblages on islands worldwide. The species pool of the null assemblages to calculate the NRI values is global (compare Fig. 1A in main text).

Island name	TDWG unit	NRI	Rank	Phylogenetic structure and composition	References
Borneo	BOR	6.26	9	Several large palm genera are represented by many species (including *Calamus*, *Daemonorops*, *Iguanura*, *Areca*, *Pinanga*, *Licuala*) and some genera are closely related within higher groups (e.g., tribes Calameae, Areceae, Trachycarpeae)	(1, 2)
Cuba	CUB	18.13	4	Palm flora dominated by major radiations in *Coccothrinax* and *Copernicia*, as well as the smaller genus *Roystonea*. Some higher lineages generally well represented (e.g., tribe Cryosophileae)	(1)
Fiji	FIJ	11.61	5	The majority of genera fall within one tribe (Areceae), with the two most diverse genera (*Balaka* and *Veitchia*) being closely related	(1)
Hawaii	HAW	20.65	3	One genus that has radiated extensively (*Pritchardia*; 22 of the 27 recognized species are Hawaiian endemics)	(1)
Madagascar	MDG	40.9	1	Spectacular radiation of the genus *Dypsis* (>140 *Dypsis* species accounting for 80% of all species). Remaining species also include the genus *Ravenea*, 16 of which are endemic to Madagascar.	(1, 3, 4)
New Caledonia	NWC	22.03	2	Apart from one species, all taxa in New Caledonia are restricted to three subtribes (Archontophoenicinae, Basseliniinae, Clinospermatinae) within the Pacific clade of tribe Areceae.	(1, 5)
New Guinea	NWG	10.78	6	Majority of genera of New Guinea palms fall within subtribe Areceae, including some significant radiations in *Heterospathe*, *Hydriastele*, *Calyptrocalyx*, and subtribe Ptychospermatinae. Important radiations also in *Calamus*, *Licuala* and *Saribus*.	(1, 2)
Lord Howe-Norfolk Is.	NFK	5.52	10	All species within Areceae, including both genera of Rhopalostylidinae (*Hedyscepe* and *Rhopalostylis*) and both species of *Howea*.	(1, 6)
Solomon Islands	SOL	8.46	7	Palm flora dominated by genera from tribe Areceae (76%)	(1, 2)
Sumatra	SUM	7.22	8	Similar to Borneo, though species diversity is lower in all groups (much lower in some cases, e.g., *Iguanura* and *Licuala*)	(1, 2)

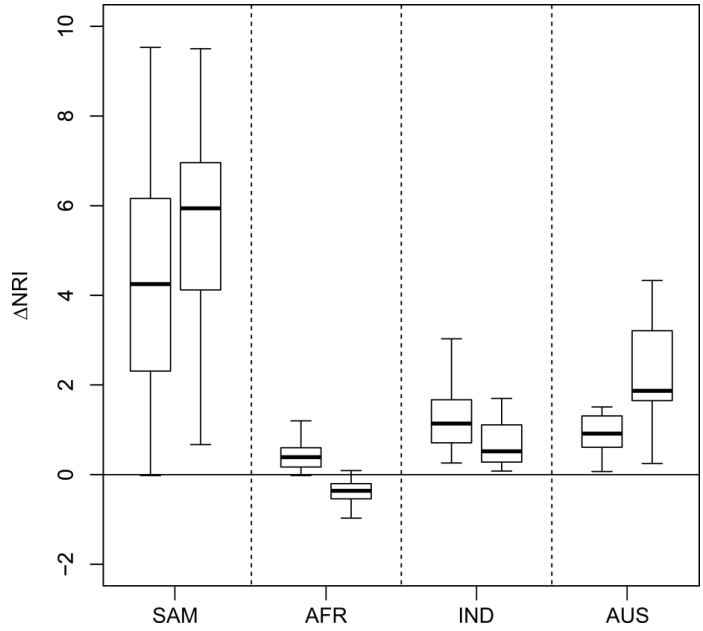

Fig. S1: Effects of sampling pool scaling on NRI within biogeographic realms (SAM = South America; AFR = Africa; IND = Indomalaya; AUS = Australasia). Within each panel, the left box plot shows the change in NRI between global and hemispheric sampling pools (i.e., $NRI_{global} - NRI_{hemispheric}$). The right box plot shows the change in NRI between hemispheric and realm sampling pools ($NRI_{hemispheric} - NRI_{realm}$). Values > 0 indicate stronger phylogenetic clustering with the geographically more extensive sampling pool. All distributions are significantly $\neq 0$ ($P \leq 0.001$) (see Table S3).

Table S3: Statistical results for testing whether changes in the mean net relatedness index (NRI) in relation to sampling pools are significantly different from zero. For each assemblage within a realm, we computed $NRI_{global\ pool} - NRI_{hemispheric\ pool}$ and $NRI_{hemispheric\ pool} - NRI_{realm\ pool}$ and used an intercept-only linear ordinary least squares (OLS) regression model to test whether the intercept significantly departs from zero (equivalent to a paired two sample *t*-test). In the presence of spatial autocorrelation in OLS model residuals, a spatial model of the simultaneous autoregressive error type (SAR) was used instead (equivalent to a 'spatial' paired two sample *t*-test). SAR model fitting and Moran's *I* calculations as in Table S1. Note that all changes in NRI values in relation to sampling pool scaling are significant.

Model				Results		
Spatial extent	Sample size	Sampling pool change	Model type	Intercept (±SE)	*z* or *t*	*P*-value
South America	17	global -> hemispheric	SAR	4.931 (±1.290)	3.824	<0.001
South America	17	hemispheric -> realm	SAR	5.797 (±1.440)	4.027	<0.001
Africa	43	global -> hemispheric	SAR	0.392 (±0.075)	5.200	<0.001
Africa	43	hemispheric -> realm	SAR	-0.419 (±0.111)	-3.786	<0.001
Indomalaya	25	global -> hemispheric	SAR	1.299 (±0.262)	4.952	<0.001
Indomalaya	25	hemispheric -> realm	SAR	0.691 (±0.121)	5.728	<0.001
Australasia	14	global -> hemispheric	OLS	1.156 (±0.266)	4.349	<0.001
Australasia	14	hemispheric -> realm	OLS	2.735 (±0.675)	4.053	0.001

Quaternary climate change

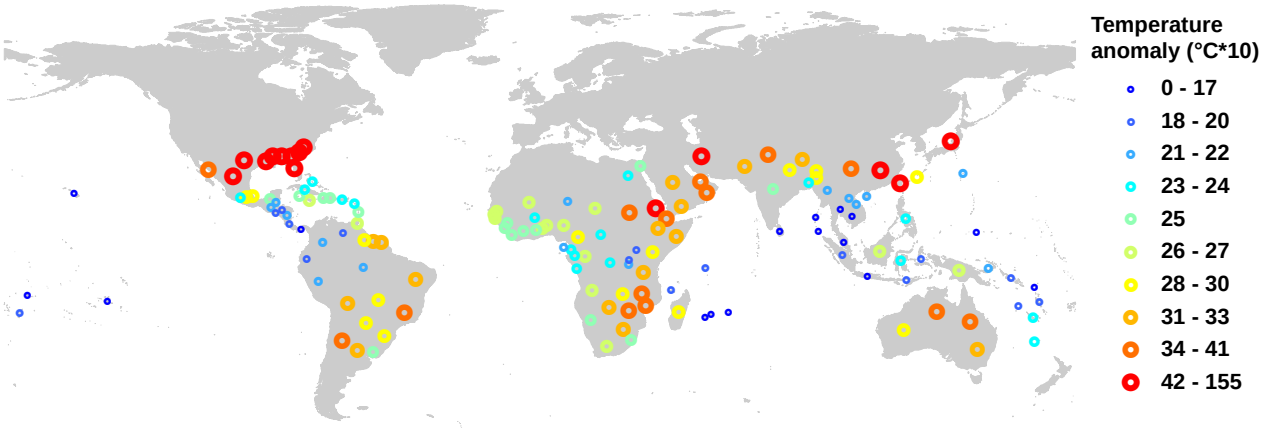

Fig. S2: Mean temperature changes (anomalies) between the Last Glacial Maximum (LGM, ca. 0.021 mya) and the present plotted for the centroid of each 'botanical country' that has more than one palm species present. Data are ensemble (means) of the temperature anomalies of two paleoclimatic simulations (CCSM3 and MIROC3.2; see methods). Classification uses quantiles and maps are in Behrmann projection.

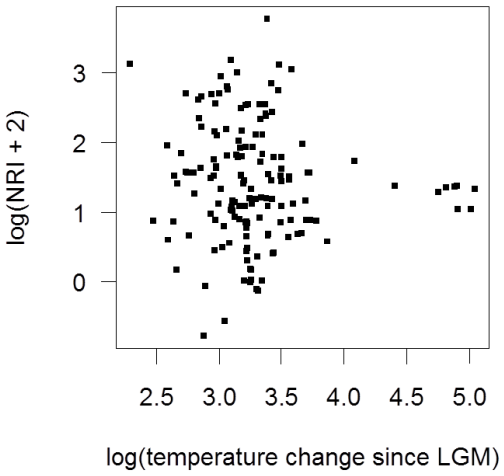

Fig. S3: Global relationship between Quaternary climatic oscillations and the net relatedness index (NRI) in palms (calculated with a global sampling pool). Quaternary climatic oscillations were quantified as the change in mean annual temperature (anomaly, in °C*10) between the Last Glacial Maximum (~0.021 mya) and the present (compare Fig. S2 and methods). The relationship between NRI and Quaternary temperature change is not statistically significant at a global scale (see Table S4 for statistical results).

Table S4: Single-predictor models of the effect of Quaternary temperature change (predictor) on the net relatedness index (NRI; response) in palms globally and within four biogeographic realms (South America, Africa, Indomalaya, and Australasia). The relationship is only significant within South America and Africa (highlighted in bold). Quaternary temperature change was quantified as the anomaly in mean annual temperature between the Last Glacial Maximum (LGM, ~0.021 mya) and the present. For the calculation of NRI values, the spatial extent of sampling pools was global for the global analysis and restricted to a continental/biogeographic scale for the realm analyses. Results from ordinary least square regression models (OLS) and spatial autoregressive error models (SAR) are given. SAR models were fitted to account for spatial autocorrelation in model residuals using a spatial weights matrix with a row standardized coding scheme (7) and a Gabriel connection (global) or a minimum distance to connect each sample unit to at least one other site (realm). The explained variance (R^2) of the SAR model includes only the environmental component to make it comparable to OLS (i.e., it excludes the explanatory power of the spatial weights matrix). Moran's *I* values quantify residual spatial autocorrelation based on the four nearest neighbors of each site. Significance of Moran's *I* statistics was determined from permutation tests (n = 1000 permutations). Sample sizes (n geographic units) are provided after the region names.

Model statistics	Global (n = 151)		South America (n = 17)		Africa (n = 43)		Indomalaya (n = 25)		Australasia (n = 14)	
	OLS	SAR	OLS	SAR	OLS	SAR	OLS	SAR	OLS	SAR
Intercept	1.891	1.524	-7.873	-4.224	-2.900	-3.040	-0.614	-0.618	0.636	-0.912
Coefficient	-0.142	-0.045	0.338	0.201	1.102	1.142	0.422	0.423	0.150	0.642
Std. Error	0.145	0.176	0.100	0.101	0.498	0.519	0.333	0.318	0.778	0.870
t or *z* value	-0.976	-0.237	3.383	1.991	2.213	2.199	1.270	1.330	0.193	0.738
P-value	0.330	0.813	**0.004**	**0.046**	**0.033**	**0.028**	0.217	0.183	0.850	0.460
R^2	0.006	0.006	0.433	0.433	0.107	0.107	0.065	0.065	0.003	0.003
Moran's *I*	0.503	0.034	0.187	0.135	0.181	0.049	-0.049	-0.049	0.093	0.041
P of Moran's *I*	<0.001	0.205	0.051	0.077	0.017	0.214	0.490	0.494	0.133	0.175

For South America, the frequency distribution of model residuals approximated a normal distribution, so data could be analyzed with untransformed variables. For the other realms and the global analysis, the response variable (NRI+2) as well as the predictor variable (Quaternary temperature change) was log-transformed.

Table S5: Coefficients from the most parsimonious multiple-predictor model to explain the net relatedness index (NRI) in palms within South America and Africa in relation to Quaternary temperature anomaly (ANOM TEMP) and present-day environment (ELEV, PREC, PREC SEAS, TEMP, TEMP SEAS). A full model with all predictor variables was subject to a step-wise model selection based on the Akaike information criterion (AIC). '–', not selected by step-wise model selection. Moran's *I* statistics indicate no spatial autocorrelation in model residuals.

	South America (*n* = 17)		Africa (*n* = 43)	
	Coefficient	*P*	Coefficient	*P*
Intercept	20.258	*	-4.571	*
ANOM TEMP	0.234	*	1.379	*
ELEV	-0.001	***	–	
PREC	-0.003	*	–	
PREC SEAS	–		-0.007	n.s.
TEMP	-0.057	*	0.006	n.s.
TEMP SEAS	-0.002	**	–	
R^2	0.840		0.191	
Moran's *I*	-0.178		0.080	
P of Moran's *I*	n.s.		n.s.	

ANOM TEMP, anomaly in temperature between Last Glacial Maximum and present (in °C * 10); ELEV, elevation range (in m); PREC, annual precipitation (in mm $year^{-1}$); PREC SEAS, precipitation seasonality measured as coefficient of variation of monthly values (in mm); TEMP, annual mean temperature (in °C * 10); TEMP SEAS, temperature seasonality measured as standard deviation of monthly means (in °C * 10).
Significance levels: ***$P < 0.001$; **$P < 0.01$; *$P < 0.05$; n.s., not significant.
NRI calculation: NRI values were calculated with a realm sampling pool.
Data transformations: Data for South America were analyzed with untransformed variables as model residuals approximated a normal distribution. For Africa, the response variable (NRI + 2) as well as the predictor variable (ANOM TEMP) was log-transformed.
Spatial autocorrelation: Moran's *I* values quantify residual spatial autocorrelation based on the four nearest neighbors of each site. Significance of Moran's *I* statistics was determined from permutation tests (*n* = 1000 permutations).

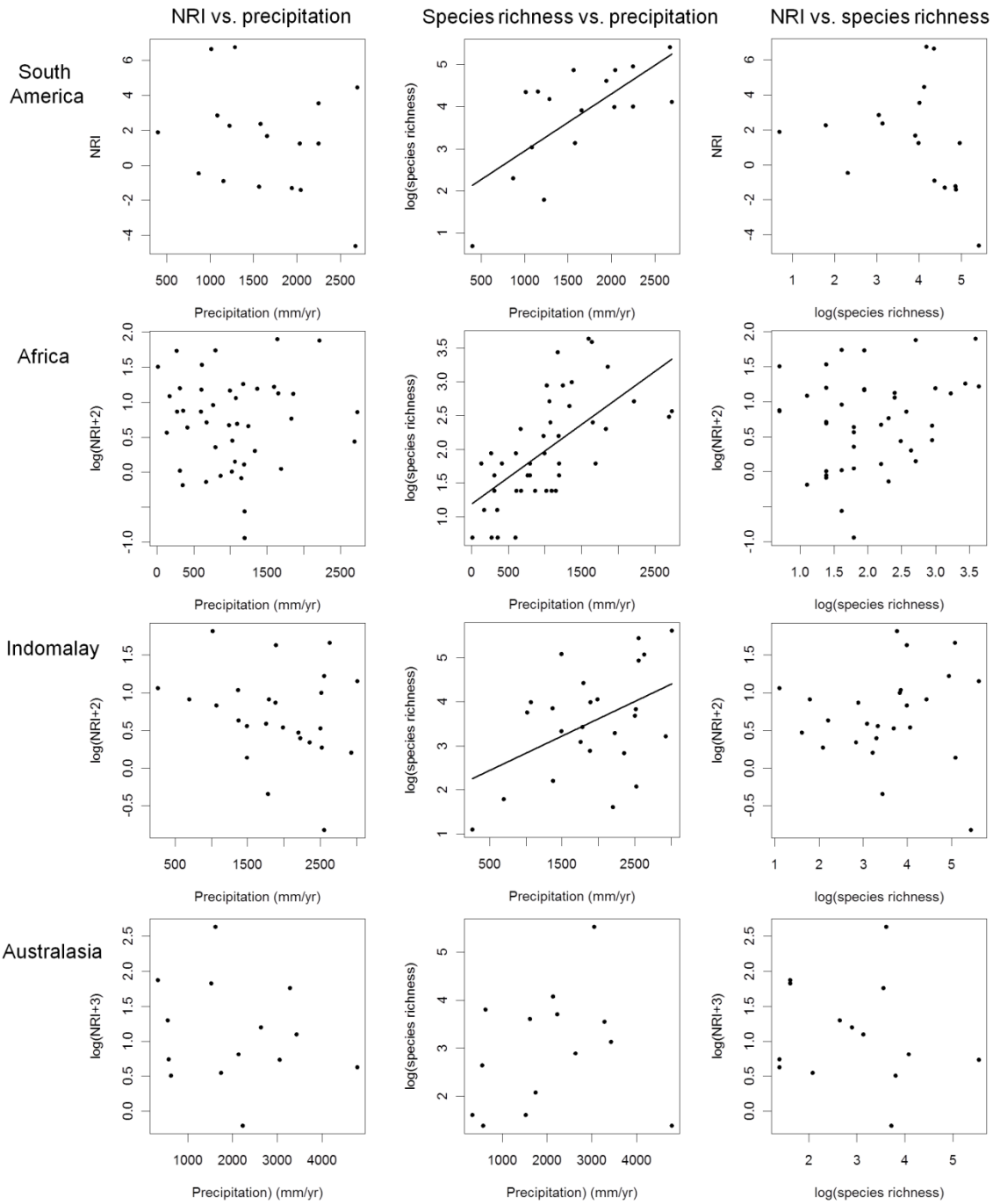

Fig. S4: The relationships between the net relatedness index (NRI), precipitation, and species richness within four biogeographic realms (South America, Africa, Indomalaya, and Australasia). For the calculation of NRI values, the spatial extent of sampling pools was restricted to a continental/biogeographic scale. Note that the commonly observed increase of species richness with precipitation is not reflected in the NRI.

Table S6: Endemism in palms at different taxonomic levels and various biogeographic scales. Data are based on the World Checklist of Palms (downloaded on 9th March 2009). Biogeographic scales (global, New World vs. Old World, and within four realms) correspond to Fig. 1 in the main text. Taxonomic levels distinguish species, genera and tribes. Note the extremely high level of endemism at the species level, but also the high degree of endemism at the tribe level in the New World and the Old World.

	Species			Genus			Tribe		
Biogeographic scale	Endemic	Total	Percent	Endemic	Total	Percent	Endemic	Total	Percent
Global	2440	2440	100.0	183	183	100.0	29	29	100
New World	782	784	99.7	65	69	94.2	11	17	64.7
Old World	1656	1658	99.8	114	118	96.6	12	18	66.7
South America	371	451	82.2	17	51	33.3	1	15	6.7
Africa	50	65	76.9	5	16	31.3	1	9	11.1
Indomalay	872	897	97.2	23	46	50.0	1	12	8.3
Australasia	451	472	95.6	28	56	50.0	0	11	0.0

Text S1: Dispersal and phylogenetic assemblage structure in palms

Most palm species have limited capacities for long-distance dispersal via oceanic drift because floating seeds, though well known, are the exception (notably *Cocos nucifera* and *Nypa fruticans*) (1). Instead, palm seeds are generally heavy, dense, and most commonly sink. Palm fruits are mostly dispersed by small- to large-bodied frugivorous birds and mammals (8, 9) and fruit sizes typically range between 1–3 cm (Fig. S5). Nevertheless, a few palm genera (e.g., *Lodoicea*, *Cocos* and *Borassus*) have large fruits (e.g., >10 cm). As a consequence of seed dispersal by birds and mammals, palm fruits are mostly dispersed at short to medium distances (<100 km; (10)) while seed dispersal among continents and realms is apparently very rare. The limited long-distance dispersal capacity of most palms is reflected in a high degree of endemism (Table S6) and in the fact that only few palm genera (*Elaeis* and *Raphia*) are present at both sides of the Atlantic (in Africa and South America). Of the 2,440 palm species analyzed in this study a total of 1,648 (68%) occur in only one of the level 3 geographic units ("botanical countries") of the World Geographical Scheme for Recording Plant Distributions. Moreover, there is not only an extremely high degree of endemism at the species level in all realms, but also a high degree of endemism at the tribe level in the New World and the Old World (Table S6). Overall, this limited transoceanic dispersal capacity (together with *in situ* diversification) results in pronounced phylogenetic clustering of regional palm assemblages in South America, Indomalaya, and Australasia when using a global (or New World vs. Old World) species pool for NRI calculations (Fig. 1 and Fig. 2 in main text).

Beyond cross-continental dispersal limitation, phylogenetic clustering in palms might also be influenced by dispersal processes within realms. Notably, strong dispersal limitation (for both seeds and pollen) is likely to increase speciation because intraspecific gene flow at the population level is low (11). Two basic traits in particular may influence dispersal limitation in animal-dispersed plants, namely stem height and fruit (seed) size (12-14). If stem height of fleshy-fruited plants is small, such as in understory palms, the sedentary nature of most frugivorous birds in the understory of tropical rainforests has been proposed to lead to strong dispersal limitation at the local or landscape scale (11). Empirical evidence supports this idea for palms, as understory palms show a stronger decay with environmental and geographical distance than canopy palms (15), suggesting that the former might be more dispersal limited than the latter. The high species diversity of some palm genera in the understory of tropical rainforests (e.g., *Bactris* (16), *Chamaedorea* (17), and *Geonoma* (18) in South America) and its spatial congruence with high phylogenetic clustering is consistent with this hypothesis. Besides stem height, fruit size may also influence dispersal limitation in palms, e.g., by shaping dispersal mode. Fleshy fruits of ≥4 cm are often predominantly dispersed by non-flying mammals, including scatter-hoarding rodents, primates, elephants, and tapirs (8, 19, 20). However, non-flying mammals are less effective than flying animal dispersers (birds and bats) for seed dispersal across major barriers (rivers, mountain ranges, or vast stretches of sea). This has been demonstrated empirically by studying the colonization of volcanic islands (e.g., Krakatau or Long Island) through palms (21) and other fleshy-fruited plants (22, 23). Hence, the presence, abundance and predominance of flying vs. non-flying dispersers could have important consequences for allopatric speciation and phylogenetic clustering within realms.

Comparing fruit sizes and stem heights of palms across realms (Fig. S5) suggests that Africa generally shows a paucity of small-fruited palms, both in short-statured species (stem heights <15 m) as well as tall-statured species. Instead, the African palm flora is dominated by large-fruited palms (Fig. S5) which are often dispersed by non-flying mammals (8). The paucity of small-fruited palms in Africa (including both short-stemmed and tall-growing species) may be related to the

drying of this region during the Cenozoic (Fig. 3*A* in main text) because a larger seed mass enables seedlings to better survive hazards such as drought (24) and because tropical rainforest understory plants are especially sensitive to drought (25). Hence, the dramatic drying of Africa during the Cenozoic could have had a strong effect on dispersal trait composition of palm species assemblages in this region. However, it remains unclear to what extent seed dispersal of non-flying mammals affects speciation and phylogenetic structuring of fleshy-fruited plants, e.g., relative to seed dispersal by birds and bats or when considering seed dispersal services of extinct megafauna (26).

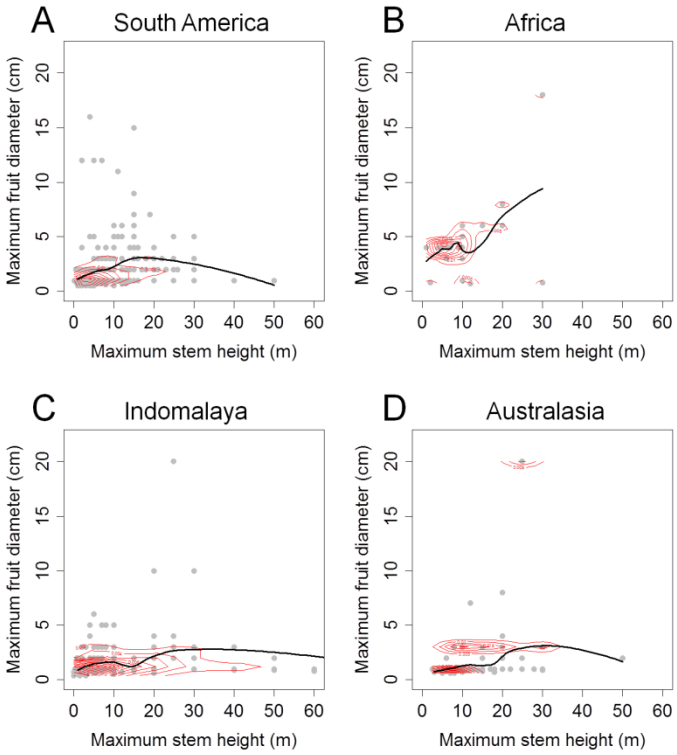

Fig. S5: Plots of fruit size vs. stem height for palm species in (*A*) South America (*n* = 295), (*B*) Africa (*n* = 25), (*C*) Indomalaya (*n* = 204), and (*D*) Australasia (*n* = 90). Note that Africa generally misses small-fruited palms (< 4cm fruit diameter), both short-stemmed as well as tall-stemmed species. Red contour lines indicate two-dimensional kernel densities as derived from the R function kde2d(). The black lines represent local polynomial regression fits as obtained from the R function loess(). Data were obtained from (9). This data source provides information on fruit size and stem height for >1,100 palm species (45%). Only those species were included which occur within the four realms and for which data on both fruit size and stem height were available.

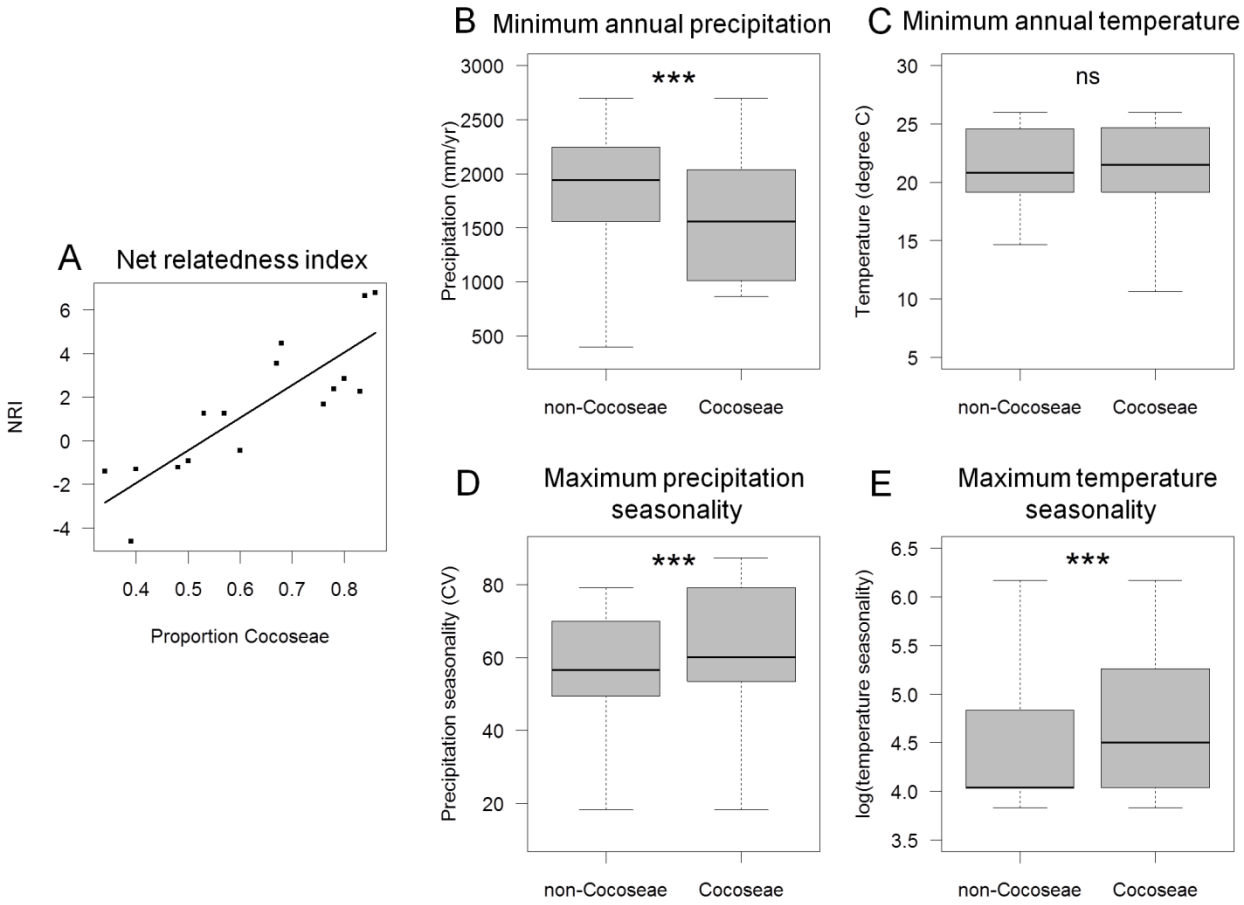

Figure S6: The Cocoseae effect in South America. (*A*) Relationship between the net relatedness index (NRI) and the proportion of species in the tribe Cocoseae within TDWG level 3 units (R^2 = 0.72, P<0.001), and (*B-E*) boxplots of species-climate sensitivities compared for species within the tribe Cocoseae vs. the rest. In (*B-E*), the minimum (*B,C*) or maximum (*D,E*) country-level climate mean value for each species within its geographic range (based on occurrences within level 3 geographic units of the World Geographical Scheme for Recording Plant Distributions) was taken to indicate species-level climatic sensitivity. Seasonality values (*D,E*) were quantified as coefficient of variation (CV) of monthly precipitation values and standard deviation (SD) of monthly temperature values. T-tests were used to compare differences in mean climate sensitivities between Cocoseae and non-Cocoseae species. NRI is largely driven by the proportion of species within the tribe Cocoseae. Cocoseae species tend to occur in areas that are drier and have higher precipitation and temperature seasonalities than areas were non-Cocoseae species occur. The strong correlation between NRI and Quaternary temperature anomaly (Spearman rank: r = 0.67, see also Fig. 5*A* main text) becomes weak once the proportion of Cocoseae species has been accounted for (partial Spearman rank: r = 0.34).

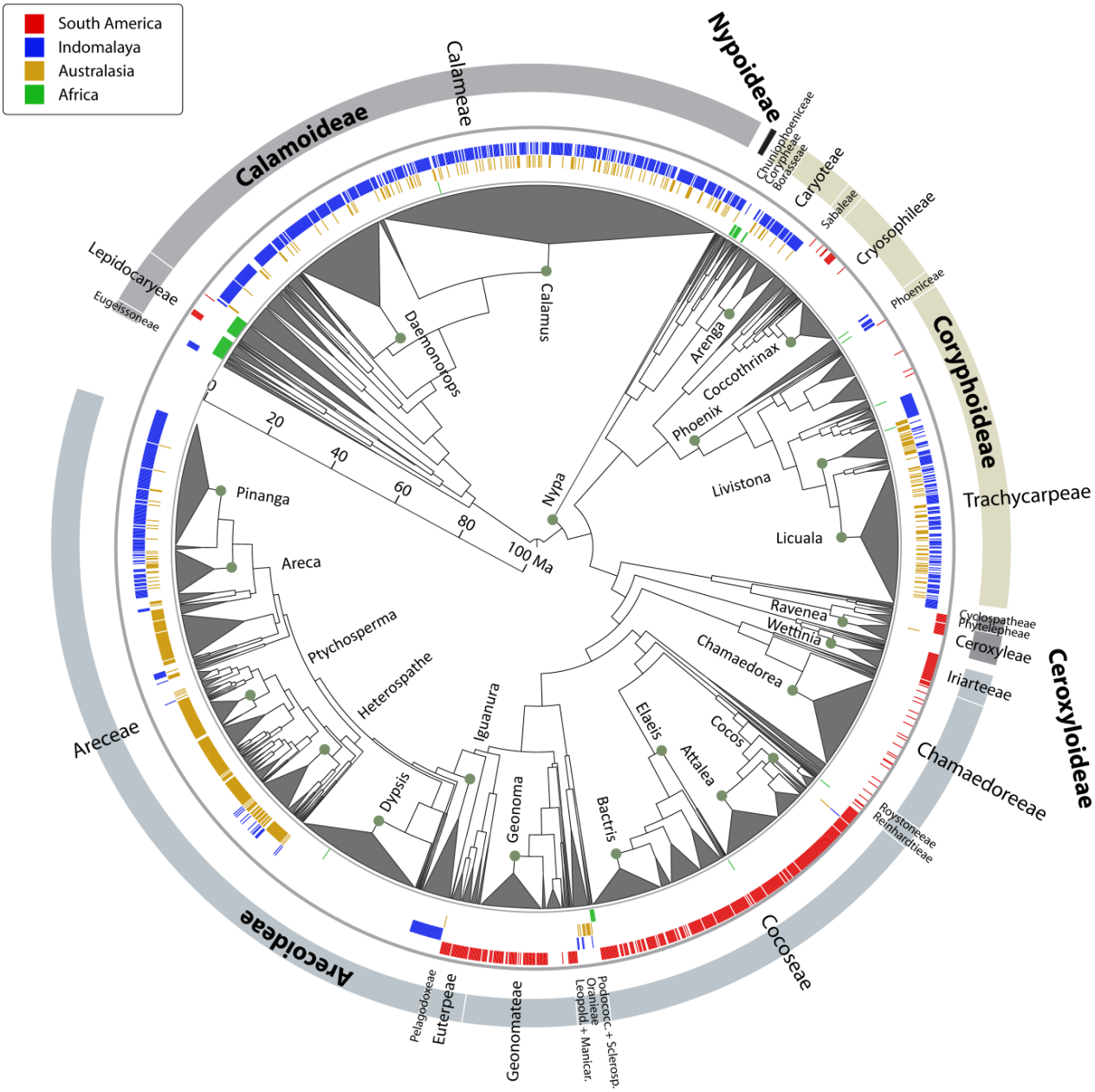

Fig. S7: The phylogenetic tree used in this study. The tree is based on a dated version (27) of a recent supertree of all palm genera, the most extensive phylogenetic study of the palm family published to date (28). Below the genus level, species were appended as polytomies with a divergence age arbitrarily set at two-thirds the stem node age of the genus. The width of the triangles corresponds to the number of species per genus. The time scale is in millions of years (Ma). The stem nodes of selected species-rich genera are indicated in the figure by a green dot adjacent to the generic name. Subfamilies (names in bold ending on -oideae) are separated by thick white lines in the outer gray ring. Tribes with 25 or more species (names ending in -eae) are delimited by thin white lines in the outer gray ring. Names of tribes are printed in a font size proportional to their size (smallest font 0–24 species; medium font 25–99 species; largest font > 100 species). Colors in the inner rings correspond to species occurring in the four biogeographic realms (South America, Indomalaya, Australasia, Africa) as used in this study (compare Fig. 1*C* in main text). Note that species within genera are ordered randomly. Species with no colour are found outside the four biogeographic realms in Fig. 1*C*, e.g., Madagascar (e.g., *Dypsis*), Central or North America, the Carribean (e.g., *Coccothrinax*), or the Pacific Islands.

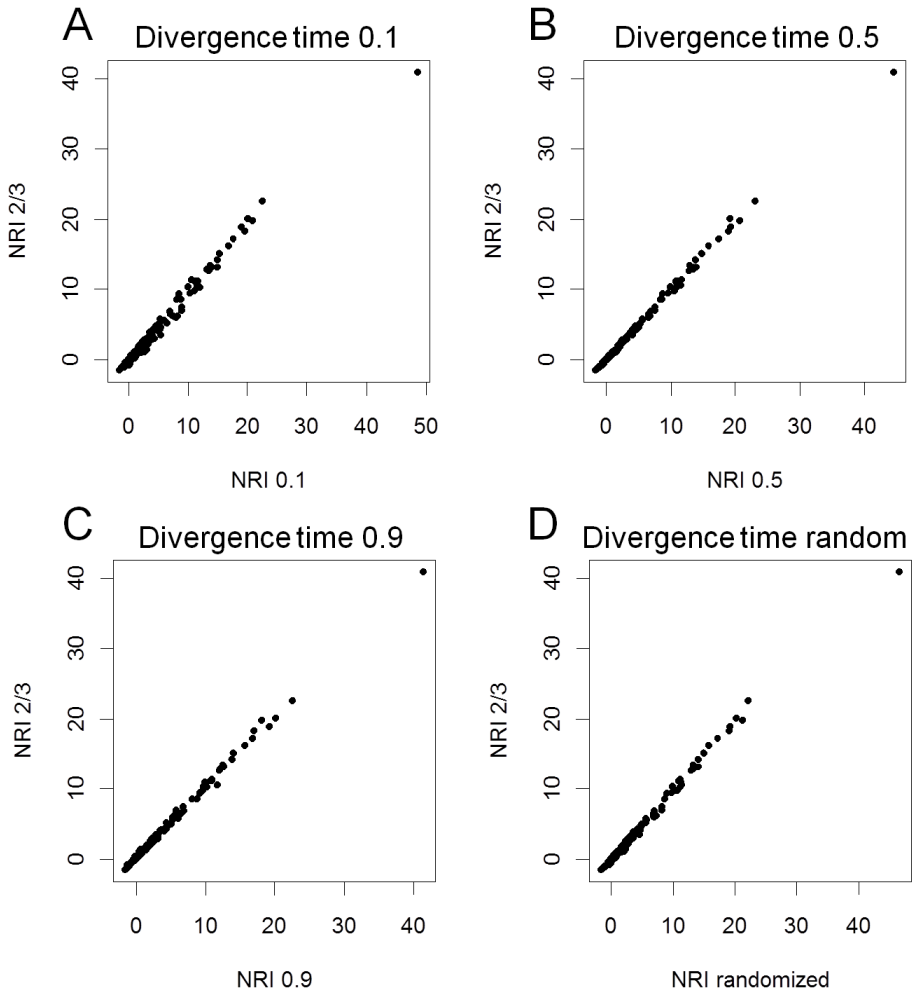

Fig. S8: Influence of the assumed divergence time among species within genera on the net relatedness index (NRI). In all cases, NRI was calculated on the same set of palm assemblages (n = 151 level 3 geographic units of the World Geographical Scheme for Recording Plant Distributions). The y-axis "NRI 2/3" represents NRI values calculated with a divergence time arbitrarily set at two-thirds of the stem node age of the genus (used throughout the paper). These values are compared to NRI values where divergence times within genera were assigned at (*A*) 0.1, (*B*) 0.5, and (*C*) 0.9 times the stem node of the genus, and (*D*) a random fraction between 0 and 2/3 of the stem node age of the genus. Note that intra-generic relationships are unresolved and thus a single divergence time per genus is used. For the calculation of (*D*), NRI calculation was repeated and averaged for 100 phylogenetic trees with randomly assigned divergence times. Note that NRI values from all these different approaches are highly correlated (all Pearson correlations $r > 0.99$). This sensitivity analysis shows that NRI calculations are robust to changing assumed divergence times within genera. This is expected because NRI values reflect deeper divergences in a phylogeny, not the shallow divergences of species within genera.

Text S2: Biome reconstructions and area-time plots

We used biome reconstructions of the tropical rainforest biome (Table S7) to estimate the available area of suitable habitat for palms since the Eocene (ca. 55 mya). We chose three reconstructions (29-31) for the deeper time periods (Eocene, Oligocene, Miocene) and used an ensemble (i.e., the average) to account for uncertainty of reconstructions during these time periods. The Eocene-to-Miocene biome reconstructions are primarily based on fossil records and palynological data and have partly been used to assess the time-integrated area effect for the latitudinal gradient in tree diversity (32). Other interpretations of the history of tropical regions (e.g., (33, 34) during these time periods rely primarily on geological data (evaporites and coal deposits) and do not explicitly reconstruct the tropical rainforest biome (32). For the more recent time periods we used reconstructions for the Middle Pliocene (35) and the Last Glacial Maximum (36) which were derived from new global biome reconstructions based on paleobotanical data and dynamic global vegetation models. The present-day distribution of tropical rainforests was based on global maps of broad vegetation types (37). The details of the sources for biome reconstructions are listed in Table S7.

Table S7: Details of sources for biome reconstructions of the tropical rainforest biome during different geological time periods.

Source	Time periods	Definition of tropical rainforest biome
(29)	Early Eocene (54–49 Mya), Oligocene (35–25 Mya), Miocene (16–10 Mya)	Closed-canopy tropical rain forests
(30)	Early Eocene (54–49 Mya), Oligocene (35–25 Mya), Miocene (16–10 Mya)	Closed canopy megathermal rainforests
(31)	Eocene (60–50 Mya), Oligocene (~30 Mya), Miocene (11.2–5.3 Mya)	Tropical everwet and subtropical summerwet forests
(35)	Middle Pliocene (3.6–2.6 Mya)	Tropical forests
(36)	Last Glacial Maximum (0.021 Mya)	Tropical forests
(37)	Present-day (0 Mya)	Tropical & subtropical moist broadleaf forests

Note: Time ranges are given for each map from each source (Mya = million years ago).

We scanned and georeferenced all maps from the biome reconstructions (see above) and digitized the rainforest areas using ArcGIS 9.3. Maps were projected to Behrmann projection to calculate the area of the rainforest polygons for each time period. From these maps we derived area-time plots for each of four biogeographic regions (South America, Africa, Indomalaya, Australasia) by plotting the area of tropical rainforests against geological time (Fig. 3 in main text). For the Early Eocene, Oligocene, and Miocene we used an ensemble (i.e., average) across the three available sources (29-31) to account for uncertainty in reconstructions. The time estimates for these periods were set to 55 Mya, 30 Mya, and 11 Mya, respectively. From the area-time plots we estimated (1) the area under the curve (AUC) as a summary statistic for the available biome area over geological time (*sensu* (32)), (2) the total loss of tropical rainforest area (Eocene minus Present), (3) the rate of habitat loss measured as the slope β of a simple linear regression of area vs. time, and (4) the minimum rainforest area available during the Cenozoic. All composite measures plus the available area of tropical rainforests during these time periods are provided in Table S8.

Table S8: Estimates of tropical rainforest area over geological time (from the Eocene to the present) for four major biogeographic regions. Four composite measures of tropical forest change over geological time are provided with (1) the time-integrated area measured as area under the curve (AUC), (2) the total loss of tropical rainforest area (Eocene minus Present), (3) the rate of habitat loss measured as the slope β of a simple linear regression of area vs. time, and (4) the minimum rainforest area available during the Cenozoic.

	Area of tropical rainforest biome (in 1,000 km^2)						Time-integrated area (AUC)	Total area loss (in 1,000 km^2)	Rate of area loss (slope β)	Minimum area (in 1,000 km^2)
Region	Eocene	Oligocene	Miocene	Pliocene	LGM	Present				
South America	12,902	8,804	8,498	8,984	8,123	8,569	1,118	4,333	0.071	8,123
Africa	21,640	16,263	15,457	9,530	3,925	3,149	1,419	18,491	0.298	3,149
Indomalay	8,762	7,155	6,945	4,267	3,149	5,889	709	2,873	0.078	3,149
Australasia	7,232	3,422	4,390	2,167	927	1,154	353	6,078	0.098	927

Note: Composite measures of tropical rainforest change over geological time were derived from area-time plots (*sensu* (32)) which plot biome area versus geological time (compare Fig. 3 in main text).

References

1. Dransfield J, *et al.* (2008) *Genera palmarum - the evolution and classification of palms* (Royal Botanical Gardens, Kew).
2. Baker WJ & Couvreur TLP (in press) Biogeography and distribution patterns of Southeast Asian palms. *Biotic evolution and environmental change in Southeast Asia*, eds Gower D, Johnson K, Richardson JE, Rosen B, Rüber L, & Williams S (Cambridge University Press, Cambridge).
3. Dransfield J & Beentje H (1995) *The palms of Madagascar* (Royal Botanic Gardens Kew and The International Palm Society, Kew).
4. Rakotoarinivo M (2010) New species of *Dypsis* and *Ravenea* (Arecaceae) from Madagascar. *Kew Bulletin* 65(2):279-303.
5. Pintaud J-C & Baker WJ (2008) A revision of the palm genera (Arecaceae) of New Caledonia. *Kew Bulletin* 63(1):61-73.
6. Savolainen V, *et al.* (2006) Sympatric speciation in palms on an oceanic island. *Nature* 441(7090):210-213.
7. Kissling WD & Carl G (2008) Spatial autocorrelation and the selection of simultaneous autoregressive models. *Global Ecology and Biogeography* 17(1):59-71.
8. Zona S & Henderson A (1989) A review of animal mediated seed dispersal of palms. *Selbyana* 11:6-21.
9. Henderson A (2002) *Evolution and ecology of palms* (The New York Botanical Garden Press, Bronx).
10. Holland RA, Wikelski M, Kummeth F, & Bosque C (2009) The secret life of oilbirds: new insights into the movement ecology of a unique avian frugivore. *Plos One* 4(12).
11. Givnish TJ (2010) Ecology of plant speciation. *Taxon* 59(5):1326-1366.
12. Lord JM (2004) Frugivore gape size and the evolution of fruit size and shape in southern hemisphere floras. *Austral Ecology* 29(4):430-436.
13. Muller-Landau HC, Wright SJ, Calderón O, Condit R, & Hubbell SP (2008) Interspecific variation in primary seed dispersal in a tropical forest. *Journal of Ecology* 96(4):653-667.
14. Jordano P (1995) Angiosperm fleshy fruits and seed dispersers - a comparative analysis of adaptation and constraints in plant-animal interactions. *American Naturalist* 145(2):163-191.
15. Kristiansen T, *et al.* (in press) Environment versus dispersal in the assembly of western Amazonian palm communities. *Journal of Biogeography* doi:10.1111/j.1365-2699.2012.02689.x.
16. Henderson A (2000) *Bactris* (Palmae). *Flora Neotropica Monographs* 79:1-181.
17. Hodel DR (1992) *Chamaedorea palms: the species and their cultivation* (The International Palm Society, Allen Press, Lawrence, Kansas).
18. Henderson A (2011) A revision of *Geonoma* (Arecaceae). *Phytotaxa* 17:1–271.
19. Guimarães Jr PR, Galetti M, & Jordano P (2008) Seed dispersal anachronisms: rethinking the fruits extinct megafauna ate. *Plos One* 3(3):e1745.
20. Galetti M, Keuroghlian A, Hanada L, & Morato MI (2001) Frugivory and seed dispersal by the Lowland Tapir (*Tapirus terrestris*) in Southeast Brazil. *Biotropica* 33(4):723-726.
21. Morici C (2004) Palmeras e islas: la insularidad en una de las familias mas diversas del reino vegetal. *Ecologia Insular*, eds Fernandez-Palacios JM & Morici C (Asociacion Española de Ecología Terrestre, Badajoz), pp 81-122.
22. Thornton IWB, Compton SG, & Wilson CN (1996) The role of animals in the colonization of the Krakatau Islands by fig trees (*Ficus* species). *Journal of Biogeography* 23:577-592.
23. Shanahan M, Harrison RD, Yamuna R, Boen W, & Thornton IWB (2001) Colonization of an island volcano, Long Island, Papua New Guinea, and an emergent island, Motmot, in its caldera lake. V. Colonization by figs (*Ficus* spp.), their dispersers and pollinators. *Journal of Biogeography* 28(11-12):1365-1377.
24. Westoby M, Leishman M, & Lord J (1996) Comparative ecology of seed size and dispersal. *Philosophical Transactions of the Royal Society of London Series B-Biological Sciences* 351(1345):1309-1317.
25. Wright SJ (1992) Seasonal drought, soil fertility and the species density of tropical forest plant communities. *Trends in Ecology and Evolution* 7(8):260-263.

26. Hansen DM & Galetti M (2009) The forgotten megafauna. *Science* 324(5923):42-43.
27. Couvreur TLP, Forest F, & Baker WJ (2011) Origin and global diversification patterns of tropical rain forests: inferences from a complete genus-level phylogeny of palms. *BMC Biology* 9(1):44.
28. Baker WJ, *et al.* (2009) Complete generic-level phylogenetic analyses of palms (Arecaceae) with comparisons of supertree and supermatrix approaches. *Systematic Biology* 58(2):240-256.
29. Morley RJ (2000) *Origin and evolution of tropical rain forests* (John Wiley & Sons, Chichester).
30. Morley RJ (2007) Cretaceous and Tertiary climate change and the past distribution of megathermal rainforests. *Tropical rainforest responses to climate change*, eds Bush MB & Flenley JR (Springer, Berlin), pp 1-31.
31. Willis KJ & McElwain JC (2002) *The evolution of plants* (Oxford University Press, Oxford).
32. Fine PVA & Ree RH (2006) Evidence for a time-integrated species-area effect on the latitudinal gradient in tree diversity. *American Naturalist* 168(6):796-804.
33. Scotese CR (2003) *PALEOMAP project. http://www.scotese.com.*
34. Ziegler A, *et al.* (2003) Tracing the tropics across land and sea: Permian to present. *Lethaia* 36(3):227-254.
35. Salzmann U, Haywood AM, Lunt DJ, Valdes PJ, & Hill DJ (2008) A new global biome reconstruction and data-model comparison for the Middle Pliocene. *Global Ecology and Biogeography* 17(3):432-447.
36. Prentice IC, Harrison SP, & Bartlein PJ (2011) Global vegetation and terrestrial carbon cycle changes after the last ice age. *New Phytologist* 189(4):988-998.
37. Olson DM, *et al.* (2001) Terrestrial ecoregions of the world: a new map of life on earth. *Bioscience* 51(11):933-938.